

# Understanding the Structure of Amorphous Thin Film Hafnia

Andre Miranda<sup>1</sup>

<sup>1</sup> *Stanford Synchrotron Radiation Lightsource, SLAC National Accelerator Laboratory,*

*Menlo Park CA 94025*

## I. Abstract

Hafnium Oxide (HfO<sub>2</sub>) amorphous thin films are being used as gate oxides in transistors because of their high dielectric constant ( $\kappa$ ) over Silicon Dioxide. The present study looks to find the atomic structure of HfO<sub>2</sub> thin films which hasn't been done with the technique of this study. In this study, two HfO<sub>2</sub> samples were studied. One sample was made with thermal atomic layer deposition (ALD) on top of a Chromium and Gold layer on a silicon wafer. The second sample was made with plasma ALD on top of a Chromium and Gold layer on a Silicon wafer. Both films were deposited at a thickness of 50nm. To obtain atomic structure information, Grazing Incidence X-ray diffraction (GIXRD) was carried out on the HfO<sub>2</sub> samples. Because of this, absorption, footprint, polarization, and dead time corrections were applied to the scattering intensity data collected. The scattering curves displayed a difference in structure between the ALD processes. The plasma ALD sample showed the broad peak characteristic of an amorphous structure whereas the thermal ALD sample showed an amorphous structure with characteristics of crystalline materials. This appears to suggest that the thermal process results in a mostly amorphous material with crystallites within. Further, the scattering intensity data was used to calculate a pair distribution function (PDF) to show more atomic structure. The PDF showed atom distances in the plasma ALD sample had structure up to 10 Å, while the thermal ALD sample showed the same structure below 10 Å. This structure that shows up below 10 Å matches the bond distances of HfO<sub>2</sub> published in literature. The PDF for the thermal ALD sample also showed peaks up to 20 Å, suggesting repeating atomic spacing outside the HfO<sub>2</sub> molecule in the sample. This appears to suggest that there is some crystalline structure within the thermal ALD sample.

## II. INTRODUCTION

Hafnium Oxide (HfO<sub>2</sub>) has been used as a gate oxide in transistors because of its high- $\kappa$  value and low leakage current as an amorphous thin film.<sup>1</sup> The use of amorphous materials is better in gate oxides as the lack of grain boundaries allow for a high breakdown voltage versus crystalline films. The standard way to make HfO<sub>2</sub> thin films is through the atomic layer deposition (ALD) technique because it deposits an amorphous film. There are two ways of doing this deposition, thermal ALD and plasma ALD. This study aims to apply a novel approach to understand the atomic structure of the amorphous thin film HfO<sub>2</sub> samples. By doing this we can achieve rational optimization over the current Edisonian optimization. This will also help to get better cost versus performance information about the different ALD processes. This approach is using grazing incidence X-ray Scattering to get a scattering intensity curve. This curve will then be used to calculate a pair distribution function that will give the atomic spacing inside of the material. This will lead to understanding the connection between its structure and its properties that make HfO<sub>2</sub> a good gate oxide.

SLAC National Accelerator Laboratory, 2575 Sand Hill Road, Menlo Park, CA 94025

*This material is based upon work supported by the U.S. Department of Energy, Office of Science, Office of Workforce Development for Teachers and Scientists (WDTS) under the Science Undergraduate Laboratory Internship (SULI) program, under Contract No. DE-AC02-76SF00515.*

### III. EXPERIMENTAL DETAILS

#### A. Making the Samples

In this study, we looked at two samples of HfO<sub>2</sub>. They were made using differing atomic layer deposition (ALD) techniques. One was made using the thermal ALD<sup>2</sup> technique and the second was made using the plasma<sup>3</sup> ALD technique. The difference in these two processes has to do with the treatment of one of the precursors. With thermal ALD both precursors are used in a high temperature chamber to drive the reaction that deposits the HfO<sub>2</sub>. With the plasma method, one of the precursors is made into a plasma before entering the chamber. Because of the high reactivity of the plasma precursor, the reaction between precursors in the chamber can occur at a much lower temperature than thermal ALD. Both these methods result in an amorphous thin film deposited on a substrate. For this study, the HfO<sub>2</sub> samples were deposited on Silicon wafers on top of a layer of chromium and gold. The HfO<sub>2</sub> layers were made to a thickness of 50 nm.

#### B. X-ray Scattering Setup

X-ray diffraction (XRD) on the two samples was done at beam line 10-2 at the Stanford Synchrotron Radiation Lightsource (SSRL) at SLAC National Accelerator Lab. The X-ray diffraction was done at a grazing incidence geometry with a beam of energy 21.5 keV. The data was collected using a point detector that is sensitive to the entire energy spectrum. This allowed us to specify the range of energies that only corresponded to elastic scattering. The detector swept from a scattering vector (Q) value of .1 to 20.1 in steps of .04 Å<sup>-1</sup>. The scattering vector is related to angle with the following equation.

$$Q = \frac{4\pi \cdot \sin(\theta)}{\lambda}$$

Where  $\theta$  is the angle of scattering and  $\lambda$  is the wavelength of the X-ray beam. For each sample, several scans were done. This was done because the scattering from amorphous thin films is of low intensity. Summing the results of all these scans after into one intensity curve helps to reduce noise in the data allowing for better analysis.

#### C. Data Corrections

Several corrections were added to the intensity data collected because of the grazing incidence geometry. These include absorption, footprint, polarization, and dead time corrections.

The absorption correction was needed to correct for the exit path of the scattering. At low scattering angles the X-rays go through a much greater area of the sample. At high scattering angles, the X-ray goes through less of the sample. This difference causes changes in the intensity of the scattering. The following equation is what was used to correct for this.

$$C_a = e^{-\mu \cdot t \left( \frac{1}{\sin(\alpha)} + \frac{1}{\sin(\theta)} \right)}$$

Where  $\mu$  is the absorption coefficient,  $t$  is the thickness of the sample,  $\alpha$  is the incidence angle of the sample, and  $\theta$  is the scattering angle.

The footprint correction is needed because of the effect of the grazing incidence geometry. The footprint corrects for the projection of the beam onto the sample and also for the projection of the detector onto the sample. At lower angles, the scattered beam is smaller, whereas at higher scattering angles the scattered beam is bigger. This results in a difference in the intensity as the detector can only detect a section of the footprint of the scattered beam. This footprint correction is being modeled with the fluorescence scattering as the amount of fluorescence seen corresponds to how much of the sample the detector sees, which can be modeled as the footprint and used to correct the scattering intensity. The fluorescence that is collected from the detector is smoothed using the Savitzky-Golay filter and this smoothed curve is used as the footprint correction,  $C_f$ .

The polarization correction was needed because of the polarization of the beam coming from the synchrotron. This polarization causes a difference in scattered intensity with angle. The following equation corrects for this.<sup>4</sup>

$$C_p = (1 - p_H) \cdot (1 - \sin(\theta)^2) + p_H$$

The dead time correction comes ( $C_D$ ) from the detector not being able to detect another event right after an event detection. This could cause errors in the intensity of the curve. The dead time correction is found by taking the ratio of the total counts the detector sees and the total photon counts coming from scattering. The intensity curve is then multiplied by the correction factor  $C$  which is shown below.

$$C = \frac{C_D}{(C_p \cdot C_f \cdot C_a)}$$

The scattering factor is applied to each scan of a sample and the corrected intensity curves are then summed to give an overall intensity curve for the sample. This was done using the GIPDF program. The program was developed as a way to apply all these corrections and sum the results of multiple scans rapidly. This program allows for future researchers not familiar with these corrections to do the same research and use the GIPDF program to correct their data.

#### **D. Pair Distribution Function**

The intensity data is then used to calculate the pair distribution function. A pair distribution function shows the average distance of atoms from a reference atom. This sort of analysis will show the atomic structure in the short and intermediate regions. This type of analysis on amorphous thin films scattering data is a new technique that is being developed. The PDF curve shows the probability of an atom being a distance from a reference atom. A peak in the curve shows high probability and a flat section shows low probability. A crystalline material will see peaks of around the same intensity out to far distances in the PDF. This is because of the order inside of crystalline materials. An amorphous material PDF will have peaks at short distances but as the distances increase there is no order in the placement of atoms in the material and so the PDF will die off. The PDF is calculated from the intensity curve with the following equation.<sup>5</sup>

$$G(r) = \frac{2}{\pi} \int_{Q=0}^{Q_{\max}} Q[S(Q) - 1] \sin(Qr) dQ$$

Where  $Q$  is the scattering vector and  $r$  is the radial distance from a reference atom. The function  $S(Q)$  is obtained from the intensity curve that was found through X-ray scattering through the following function.

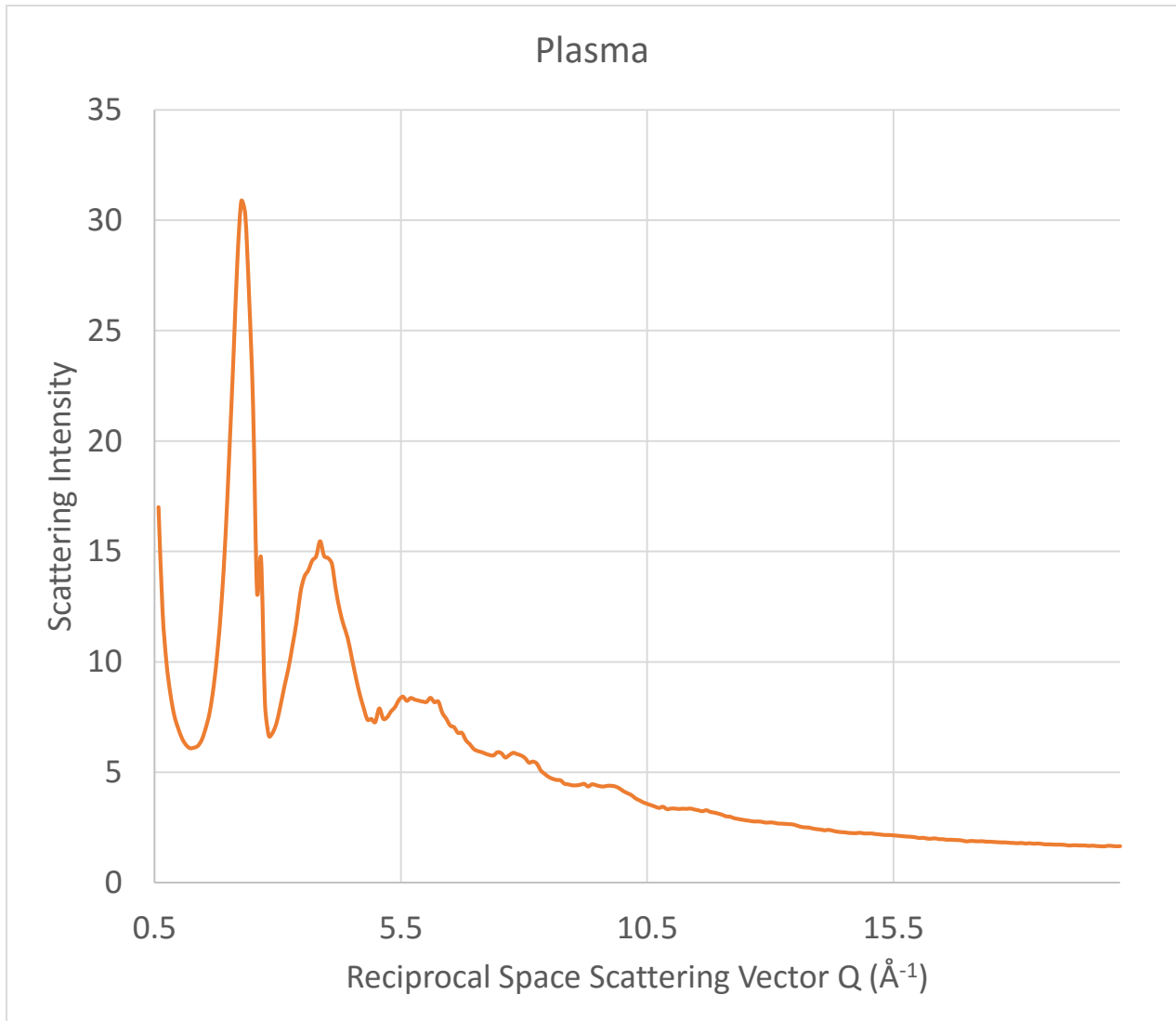
$$S(Q) = 1 + \frac{I_{el}(Q) - \sum c_i |f_i(Q)|^2}{|\sum c_i f_i(Q)|^2}$$

Where  $I_{el}$  is the intensity curve of elastic scattering,  $c_i$  is the atomic concentration, and  $f$  is the scattering factor of the sample atom or molecule. The PDF and  $S(Q)$  were calculated using PDFgetX2<sup>6</sup> software package.

#### IV. RESULTS AND DISCUSSION

##### A. Corrected Scattering Intensity

The first two figures below show the results of multiplying the correction factor to the collected scattering intensity data. Figure 1 shows the corrected intensity function for the plasma ALD sample.



The curve shows the characteristics of an amorphous structure. The curve shows distinct peaks out to a Q value of 11.5. This data suggests that the plasma ALD sample is a fully amorphous thin film.

FIG. 1 Plot of the elastic and Compton scattering against the scattering vector, Q, corrected for the corrections mentioned above. The scattering curve shows the characteristic broad peaks of an amorphous material.

Figure 2 shows the corrected intensity function of the thermal ALD sample. The broad peaks of the intensity curve also shows the characteristics of an amorphous material. This curve also shows the characteristics of crystalline materials, thin peaks in the data. Both curves' peaks occur at the same Q values suggesting that the structure of these two samples are similar despite the differences present.

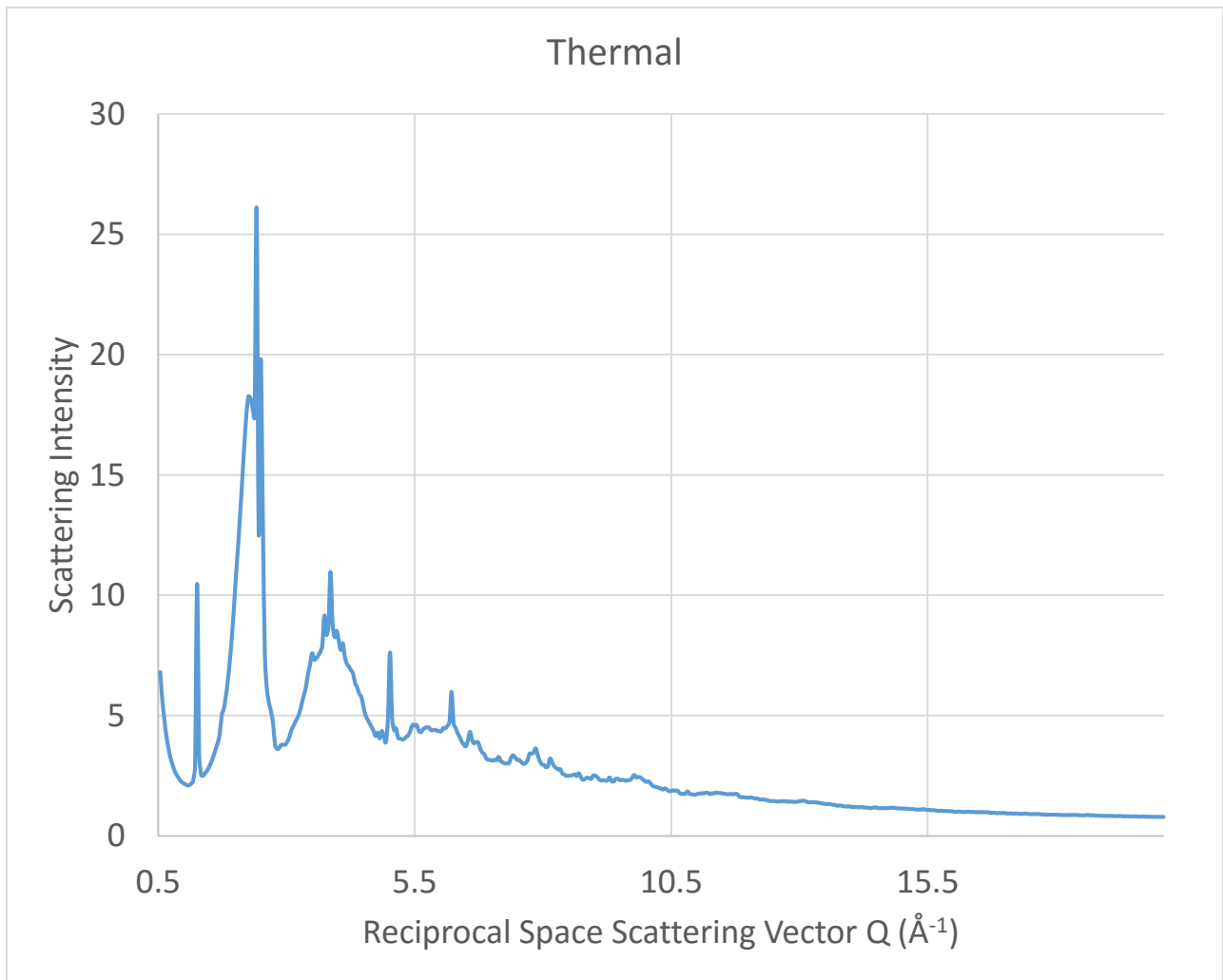


FIG. 2 Plot of the elastic and Compton scattering intensity against the scattering vector, Q, and corrected with the corrections mentioned above. Plot shows characteristic broad peaks of amorphous materials with thin peaks characteristic of crystalline material.

## B. Pair Distribution Function Calculation

The PDFs of the two samples were then calculated using the software PDFgetX2. Figure 3 shows the result of the PDF calculation for the plasma ALD sample. The plasma PDF shows peaks out to 10 Å. The first two peaks seen at 2.12 Å and 3.39 Å correspond to the bond lengths of HfO<sub>2</sub> that have been published.<sup>7-9</sup> There are two more distinct peaks in the plasma PDF before 10 Å that suggest that there is some short range order in the material for distances less than 10 Å.

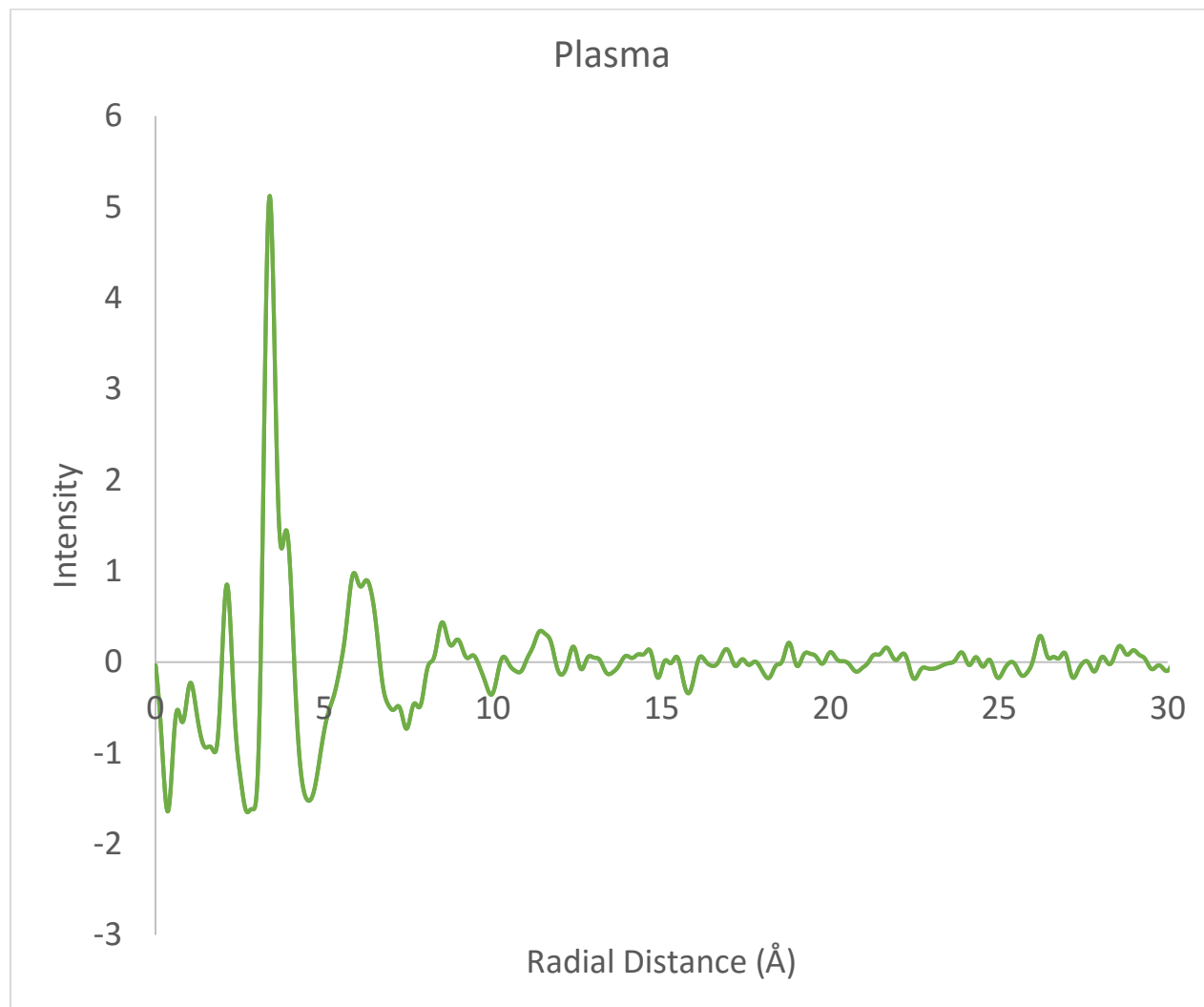


FIG. 3 Plot of the intensity of the PDF against radial distance,  $r$ , in angstroms. The first two peaks of the plot correspond to the bond lengths of the HfO<sub>2</sub> molecule and match closely the published lengths.

Figure 4 shows the thermal ALD sample PDF. The thermal PDF shows the same peak distances as the plasma between 0-10 Å. On the other hand, the thermal PDF shows distinct peaks all the way out to 20 Å. This suggests, as the scattering intensity did, that there is some crystalline structure within the thermal structure which gives rise to peaks farther out than 10 Å. The first two peaks at 2.12 Å and 3.40 Å also closely match the published<sup>7-9</sup> values for the bond lengths in HfO<sub>2</sub>.

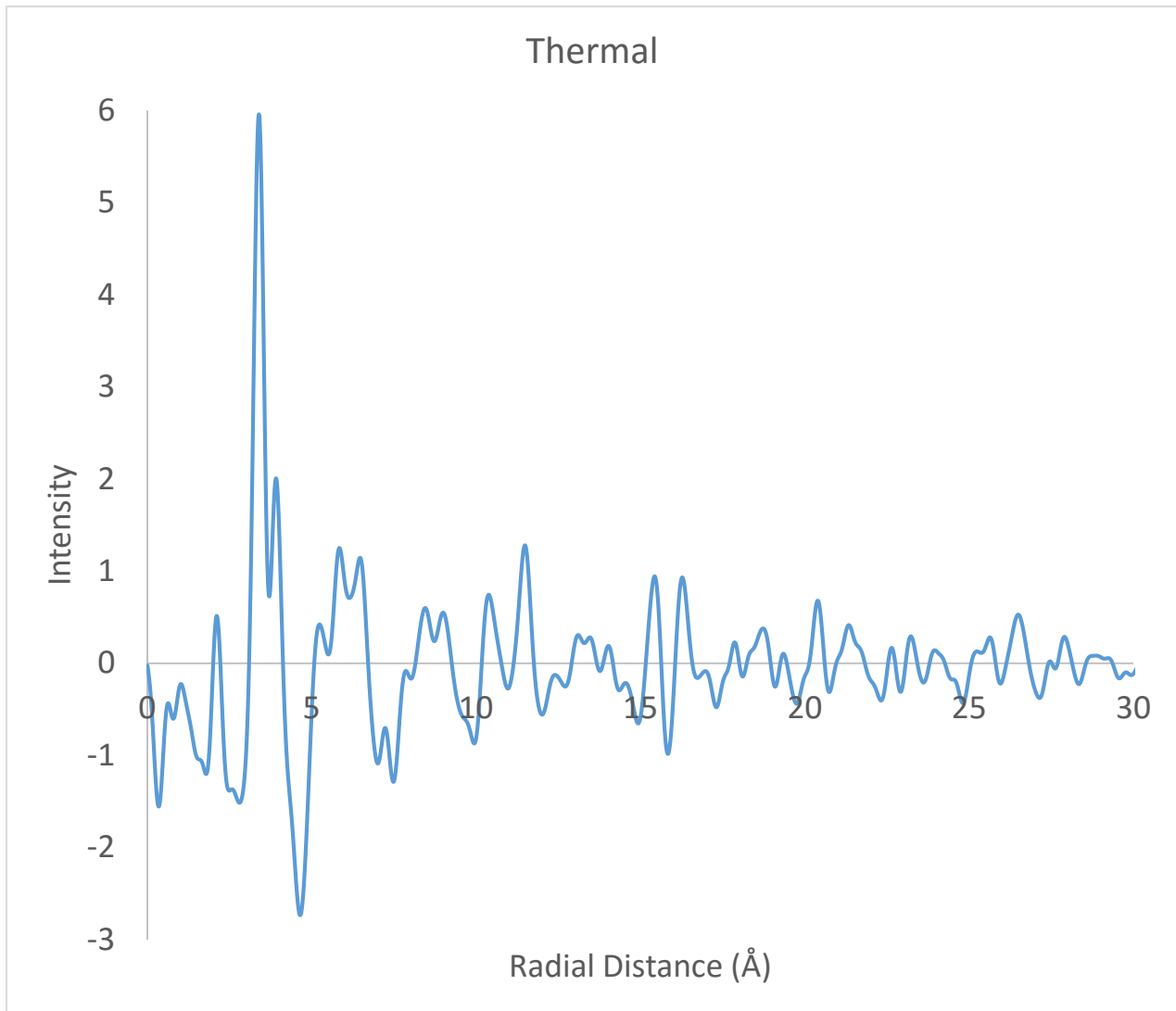


FIG. 4 Plot of the intensity of the PDF against radial distance,  $r$ , in angstroms. The first two peaks of the plot correspond to the bond lengths of the  $\text{HfO}_2$  molecule and match closely the published lengths.

## V. CONCLUSION

X-ray diffraction was used to find the atomic structure of two  $\text{HfO}_2$  samples. One of the samples was made using thermal ALD process while the second sample was made using the plasma ALD process. The scattering intensity data showed the plasma sample was fully amorphous while the thermal sample suggests it was mostly amorphous with crystallites within. This scattering intensity was then used to calculate a pair distribution function which shows atomic distances in the material. The plasma showed atomic distances out to 10 Å and flattened out after because of the disordered nature of amorphous materials. The first two peaks of the plasma ALD PDF at 2.12 Å and 3.39 Å closely match the published bond lengths of  $\text{HfO}_2$ . The thermal sample PDF showed atomic distances out to 20 Å showing more order within than the plasma suggesting crystallites within it. The first two peaks of the thermal ALD PDF at 2.12 Å and 3.40 Å also closely matches the published bond lengths of  $\text{HfO}_2$ .

Future work, we hope to perform electrical tests on both samples. This will help to see if the electrical properties change because of the structural differences that we see. We can then do more studies on samples made with the two ALD processes to see if the differences we see occur on all thermal and plasma grown amorphous thin film HfO<sub>2</sub>. Also, this study helps to show that the new method of doing X-ray scattering on amorphous thin films and getting a PDF from the intensity correctly shows the atomic structure of the thin films.

## VI. ACKNOWLEDGEMENTS

I would like to acknowledge the SSRL at SLAC National Accelerator Lab for allowing the work to be done there. Also all the helpful staff at BL 10-2 at SSRL. I'd also like to acknowledge Badri Shyam and Apurva Mehta for all their help this summer in my project. And lastly, I would like to acknowledge the DOE for this opportunity.

<sup>1</sup> Flora M. Li, Bernhard C. Bayer, Stephan Hofmann, James D. Dutson, Steve J. Wakeham, Mike J. Thwaites, William I. Milne, and Andrew J. Flewitt, *Appl. Phys. Lett.* **98**, 252903 (2011).

<sup>2</sup> Kukli, Kaupo, et al. "Atomic layer deposition of hafnium dioxide films from hafnium tetrakis (ethylmethanamide) and water." *Chemical Vapor Deposition* **8.5** (2002): 199-204.

<sup>3</sup> George, Steven M. "Atomic layer deposition: an overview." *Chemical reviews* **110.1** (2009): 111-131.

<sup>4</sup> Baker, Jessy L., et al. "Quantification of thin film crystallographic orientation using X-ray diffraction with an area detector." *Langmuir* **26.11** (2010): 9146-9151.

<sup>5</sup> Petkov, Valeri. "Atomic-Scale Structure of Glasses Using High-Energy X-Ray Diffraction." *Journal of the American Ceramic Society* **88.9** (2005): 2528-2531.

<sup>6</sup> Qiu, Xiangyun, Jeroen W. Thompson, and Simon JL Billinge. "PDFgetX2: a GUI-driven program to obtain the pair distribution function from X-ray powder diffraction data." *Journal of Applied Crystallography* **37.4** (2004): 678-678.

<sup>7</sup> Deok-Yong Cho, Tae Joo Park, Kwang Duk Na, Jeong Hwan Kim, and Cheol Seong Hwang *Phys. Rev. B* **78**, 132102 (2008).

<sup>8</sup> N. C. Das, N. K. Sahoo, D. Bhattacharyya, S. Thakur, N. M. Kamble, D. Nanda, S. Hazra, J. K. Bal, J. F. Lee, Y. L. Tai, and C. A. Hsieh, *J. Appl. Phys.* **108**, 023515 (2010).

<sup>9</sup> Patrick S. Lysaght, Joseph C. Woicik, M. Alper Sahiner, Byoung-Hun Lee and Raj Jammy, *Appl. Phys. Lett.* **91**, 122910 (2007)